



Contents lists available at ScienceDirect

Plant Science

journal homepage: www.elsevier.com/locate/plantsci



Quantitative trait loci associated with natural diversity in water-use efficiency and response to soil drying in *Brachypodium distachyon*

David L. Des Marais^{a,*},¹ Samsad Razzaque^a, Kyle M. Hernandez^{a,2}, David F. Garvin^b, Thomas E. Juenger^a

^a Department of Integrative Biology and Institute for Cell and Molecular Biology, The University of Texas at Austin, United States

^b U.S. Department of Agriculture—Agricultural Research Service, Plant Science Research Unit, St. Paul, MN, United States

ARTICLE INFO

Article history:

Received 11 January 2016

Received in revised form 18 March 2016

Accepted 23 March 2016

Available online xxx

Keywords:

Water Use Efficiency

G×E

QTL mapping

Epistasis

Abiotic stress

Brachypodium distachyon.

ABSTRACT

All plants must optimize their growth with finite resources. Water use efficiency (WUE) measures the relationship between biomass acquisition and transpired water. In the present study, we performed two experiments to understand the genetic basis of WUE and other parameters of plant-water interaction under control and water-limited conditions. Our study used two inbred natural accessions of *Brachypodium distachyon*, a model grass species with close phylogenetic affinity to temperate forage and cereal crops. First, we identify the soil water content which causes a reduction in leaf relative water content and an increase in WUE. Second, we present results from a large phenotyping experiment utilizing a recombinant inbred line mapping population derived from these same two natural accessions. We identify QTLs associated with environmentally-insensitive genetic variation in WUE, including a pair of epistatically interacting loci. We also identify QTLs associated with constitutive differences in biomass and a QTL describing an environmentally-sensitive difference in leaf carbon content. Finally, we present a new linkage map for this mapping population based on new SNP markers as well as updated genomic positions for previously described markers. Our studies provide an initial characterization of plant-water relations in *B. distachyon* and identify candidate genomic regions involved in WUE.

© 2016 Elsevier Ireland Ltd. All rights reserved.

1. Introduction

The interaction between plants and water is a critical determinant of agricultural productivity, species distribution, and ecological community assembly [1–3]. Water use efficiency (WUE) broadly describes the ratio of carbon acquired via photosynthesis to the amount of water transpired. As such, WUE reflects a key trade-off in plant growth strategy; plants may fix carbon at the biophysical limit of their photosynthetic machinery, but doing so will deplete water, a potentially finite environmental resource. Given this functional trade-off and the considerable variation in soil water availability and atmospheric evaporative demand of natural settings, it is perhaps unsurprising that diverse species of plants – and many populations within species – display substantial variation in WUE (e.g. [4–11]).

Because WUE is a ratio, variation in either the numerator – carbon assimilation – or the denominator – water consumption – can lead to WUE variation between plants or in response to environmental cues such as soil water availability. WUE can be measured in several ways [12]. Most broadly, the parameter of greatest ecological and agricultural interest is the total biomass or yield acquired per water consumed over the lifetime of a plant, termed Transpiration Efficiency, or TE [13]. However, measuring TE accurately is challenging and so several related parameters and their analytical proxies are more commonly reported and used as breeding targets. Instantaneous WUE is the leaf-level rate of carbon fixation expressed as a function of water transpired and, as such, reflects short-term physiological processes. Integrated WUE, measuring the cumulative effect of leaf-level processes over the lifetime of a measured tissue, is closely approximated by the ratio of two isotopes of carbon, ¹³C and ¹²C [14]. Abundant evidence from multiple plant species under a wide range of conditions has shown that ¹³C ratios – measured either as discrimination, Δ¹³C, or composition, δ¹³C – are a good approximation of integrated WUE for plants employing C3 photosynthesis [15]. Physiologically, the relationship between ¹³C, ¹²C, and WUE is due primarily to the preference for Rubisco to fix ¹²C, and generally accepting ¹³C more frequently when its molar ratio is elevated by partial stomatal closure and thus

* Corresponding author at: 1300 Centre St. Roslindale, MA 02131, United States.
E-mail address: desmarais@fas.harvard.edu (D.L. Des Marais).

¹ Present address: Arnold Arboretum and Department of Organismic and Evolutionary Biology, Harvard University, Cambridge, MA, United States.

² Present address: Center for Research Informatics, The University of Chicago, Chicago, IL, United States.

reduced stomatal conductance. $\Delta^{13}\text{C}$ and $\delta^{13}\text{C}$ therefore reflect the amount of carbon fixed when stomata are relatively more closed, which closely tracks WUE (and TE) in C3 plants. In the present study, we focus on $\delta^{13}\text{C}$ as a proxy for integrated lifetime WUE.

WUE is a complex trait because environmental, genetic, and developmental factors lead to variation in WUE both between and within individuals through time [16–18]. The genetic basis of WUE has been studied in several plant systems, with a general theme emerging that multiple genetic variants of small to moderate effect drive WUE differences among natural populations and among agricultural varieties of plants (e.g. [4,16,19–26]). In some cases, specific molecular variants affecting WUE have been identified; these findings reinforce the notion that genes of diverse function can drive differences in WUE. In *Arabidopsis thaliana*, the molecular basis of natural variation in WUE has been identified for three loci. These include both highly pleiotropic mutations in FRIGIDA [27] and ERECTA [28] affecting multiple whole-plant traits, as well as a WUE-reducing nucleotide variant in a MAP kinase (AtMPK12) whose apparent phenotypic effects are limited to guard cell development and environmental response [29]. Among these, AtMPK12 and FRI largely exert their effects on WUE via altered stomatal conductance whereas ERECTA affects both stomatal conductance and carbon assimilation.

Due to the strong relationship between WUE and plant performance in the field [5,11], both the genetic and physiological basis of WUE and TE in crop species are of considerable interest [13,30,31]. Using $\Delta^{13}\text{C}$ to breed for high TE has been particularly successful in rainfed Mediterranean-type agricultural settings where most precipitation occurs prior to the growing season. Reasoning that varieties which acquire more biomass per unit water consumed (high TE) should generate relatively higher yield under dry conditions than more profligate varieties, Rebetzke et al. [32] successfully used $\Delta^{13}\text{C}$ as a target of selection to increase the TE of wheat varieties and thereby realized a yield gain in water-limited environments. The yield advantage of these high-TE varieties became less pronounced as compared to traditional varieties as rainfall increased. Ecologically, the cause of this trade-off appears to be that high-TE plants grow more slowly, effectively preserving moisture stored in the soil for later in the season. When available soil water is not limiting, low-TE varieties have an advantage. It is not known which aspect of increased WUE – altered stomatal conductance or photosynthetic capacity – was targeted during this breeding process, nor is the molecular control of variation in natural variation in WUE known in any grass system. In the present study, we extend this important area of research to a model genetic system which affords the opportunity to understand the genetic basis of the trade-offs that plants experience in coordinating resource use during growth (e.g. [33]).

Brachypodium distachyon is a self-compatible, diploid, annual C3 grass native to southern Europe, north Africa, and the Middle East [34]. Abundant genetic and genomic resources are now available for *B. distachyon*, which has been developed as a model genetic system for temperate cereal crops in the Pooideae such as wheat, oat, and barley [35]. The high genomic synteny between *B. distachyon* and its Pooideae relatives [36] facilitates the translation of gene discovery in *B. distachyon* to possible improvement of cereal crops. In the present study, we contrast ecophysiological parameters of two inbred natural accessions of *B. distachyon*, Bd21 and Bd3-1, under two watering regimes. Bd21 was originally collected east of Mosul, in northern Iraq, and was the genotype sequenced to produce a reference *B. distachyon* genome sequence [36]. Bd3-1 was also originally collected in Iraq, although the exact details of its provenance are unknown [37]. A near-complete genome sequence is also available for Bd3-1 [38]. Both genotypes exhibit spring-annual life histories and do not require vernalization to initiate the

transition to flowering [39]. We first exposed Bd21 and Bd3-1 to a progressive soil drying treatment in order to identify the reduction in soil water content that causes measurable phenotypic change in plant traits. We then grew individuals from an existing Recombinant Inbred Line (RIL; [40]) mapping population to identify regions of the genome that drive constitutive differences between the two genotypes as well as regions associated with differences in soil-drying response between them. Together, these studies provide the first characterization of the genetic architecture and differentiation of Bd21 and Bd3-1 in terms of water relations and responses to moderate soil drying.

2. Methods

2.1. Assessing treatment response and genetic diversity

We planted seeds of Bd21 and Bd3-1 in Deepot D16H pots (Stuewe & Sons) filled with 250 mL of Profile porous ceramic rooting media (Profile Products). The dry weight (DW) of each pot was recorded and then plants were saturated with a 1:50 dilution of Liquid Grow Plant Food (Dyna-Gro). Pots were allowed to equilibrate to the field capacity (FC) of the soil overnight, and then weighed again. We subtracted DW from FC weight to determine the water content of each pot as the basis for the subsequent controlled soil dry down. Pots were then placed at 4 °C for 7 days to synchronize seedling germination.

All plants were grown in a Percival AR-66 growth chamber initially set to 25 °C days and 20 °C nights. Plants were watered with tap water every other day and with water supplemented with fertilizer, as above, every week. After 21 days of growth, we ramped the temperature up by 2 °C every three hours to constant 33 °C day and 25 °C night conditions. This high temperature was chosen because our prior work demonstrated that Bd21 and Bd3-1 plants have their highest seed yield under well-watered conditions at ~33 °C (Des Marais et al. in review). On the 22nd day of growth, we randomly assigned pots to control and drying treatments. Control plants were watered to 85% FC (0.54 g H₂O/g soil) every morning while dry treatment plants were allowed to dry down their pots over eight days. During the dry-down, dry treatment pots were daily brought to specified water contents such that no plant experienced greater than 10% loss of field capacity over a 24 h period.

During the dry-down, every second day we harvested four randomly-selected individuals of each genotype from each treatment (control and drying) for phenotyping. At harvest days 1 (70% FC), 4 (55% FC), 6 (45% FC), and 8 (40% FC) we harvested a single leaf from each plant and determined leaf Relative Water Content (RWC) as described previously [4]. Leaf relative water content assesses the amount of water in a leaf as a function of the maximum water content that a leaf can attain, i.e. its water content when turgid. On day 8 (30 days post-germination), we also harvested complete above- and below-ground tissue and dried these separately at 80 °C for two days. Dried tissue was weighed to determine above- and below-ground biomass, and their ratio. Complete above-ground tissues were ground to a fine powder and analyzed for $\delta^{13}\text{C}$, carbon content, and nitrogen content using mass spectrometry at the University of Georgia Analytical Chemistry Facility. Carbon isotope composition is reported relative to the PeeDee Belemnite standard, and is used rather than carbon isotope discrimination (Δ) because the isotopic composition of CO₂ in the air varies periodically in the chambers and we are principally interested in comparing relative values among samples in our experiment.

We modeled variation in leaf RWC using ANOVA with accession, treatment, harvest date, and their interaction as fixed effects using JMP Pro 10.0 (SAS Institute, Inc.). The results of this analysis indicated that our progressive soil dry-down resulted in significant

reduction in leaf RWC over time. We next modeled leaf RWC, $\delta^{13}\text{C}$, above and below-ground biomass, and leaf carbon and nitrogen content from the Day 8 harvest using ANOVA with two levels of genotype (Bd21 and Bd3-1), two levels of treatment (Control, 85% FC and Dry, 40% FC), and their interaction.

2.2. New markers and an updated linkage map for the Bd3-1 × Bd21 RIL population

We exploited a previously-generated RIL population derived from a cross between Bd3-1 and Bd21 [40]. These accessions were chosen as parents because Bd21 was the accession used to generate the reference genome [36] and because both accessions have been extensively characterized phenotypically (e.g. [38–46]). Moreover, both accessions exhibit rapid-cycling spring-annual life history strategies [39], thus reducing the time required to generate inbred lines. Development of the RIL population and some of its characteristics were described previously [40]. Individual plants representing each RIL were grown in soil in a Percival AR-66 growth chamber with 25 °C days and 20 °C nights. Plants were watered with tap water every other day and with water supplemented with fertilizer, as above, every week. After 21 days of growth, leaf tissue was harvested on liquid nitrogen and ground to a fine powder. We extracted total genomic DNA using the CTAB protocol of Kelly and Willis [47], and used the 2bRAD protocol of Wang et al. [48] to identify new markers for the RIL population. In brief, this protocol uses restriction enzymes to fractionate the genome into DNA fragments of known size and then incorporates oligonucleotide adaptors for sequencing on the SOLiD system. Sequencing was done at the University of Texas at Austin Genome Sequencing and Analysis Facility.

Raw SOLiD reads with low quality (average quality <20) or homopolymers (>20% of the read length) were filtered and converted to the fastq format (all command-line arguments used and custom scripts are available at <https://github.com/kmhernan/Publications/tree/master/DesMarais-2016-Brachy-PlantSci>). High quality reads were then aligned to the *B. distachyon* assembly v3.0 (downloaded from Phytozome on 13 August 2015) with SHRiMP v2.2.2 [49] and filtered to remove unmapped and low quality alignments with sambamba v0.5.8 [50]. The remaining alignments were further processed with the Genome Analysis Toolkit (GATK) v3.4-46-gbc02625 [51] following the Broad Institute's "Best Practices" [52] protocol. To recalibrate quality scores, an initial genotyping run was performed with GATK's UnifiedGenotyper to determine high quality SNPs (see Ref. [53]).

The GATK processed alignments were then used to detect genotypes with freebayes v0.9.21-19-gc003c1e [54]. Loci with more than two alleles and genotypes with low quality (GQ < 8) were removed using in-house scripts. The remaining genotypes were normalized using vt normalize v0.5 [55]. The normalized, bi-allelic variants were then converted to markers (hereafter referred to as "2b-RAD" data) by comparing the RIL genotypes with Bd21 (parent "A") and Bd3-1 (parent "B"). The 2b-RAD dataset was then cleaned to remove markers that exhibited segregation distortion (A/B frequencies >60%) or that had more than 30% missing data.

After filtering, the 2b-RAD markers were combined with the previously published markers (hereafter referred to as "Cui" data; [40]). First, the genomic coordinates of the Cui data were updated by aligning the flanking sequence of their previously published markers to the *B. distachyon* genome assembly v3.0 using blastn v2.2.31 [56]. The start position of the best hit for each Cui marker was extracted (if available) to determine the approximate location of the markers on the assembly v3.0. Then, both Cui and 2b-RAD data were cleaned separately by removing likely genotyping errors (e.g., variant calls that suggest double recombinants in small intervals). The cleaned 2b-RAD and Cui datasets were then merged and

redundant markers were dropped. Linkage analysis was performed on the merged markers using JoinMap 4.1 [57] using the Independence LOD thresholds of 4–10 with a step of 1. Next, marker order and distances were determined by a Maximum Likelihood mapping algorithm. Finally, recombination rates (centiMorgans, cM) were estimated using Kosambi's mapping function.

2.3. Phenotyping the Bd3-1 × Bd21 RILs and initial analyses

Ten individuals of each of 151 RILs and both parental lines were planted in a 3:1 mix of ProMix (Premier Tech) and Turface MVP (Turface Athletics) in 3.5" square pots and then cold-stratified for 7 days at 8 °C. Plants were transferred to the greenhouse facilities at the University of Texas at Austin Brackenridge Field Station in a complete randomized block design. During the initial growth phase, all plants were top-watered with dilute fertilizer, as described above. Throughout the experiment, daytime temperatures ranged from 29 to 35 °C. We did not artificially supplement the natural mid-summer sunlight in the greenhouse. On day 22 following germination, five plants of each RIL were randomly assigned to each of two treatments: control, and restricted irrigation. Control plants received 100 mL of unfertilized water every other day, while restricted irrigation plants received 50 mL of unfertilized water every other day. After 10 days of treatment, this resulted in soil water contents of 80% (Control) and 40% (Dry treatment), determined gravimetrically on the off-watering days. These treatment levels were maintained for 30 days.

We phenotyped and harvested plants on the 52nd–54th day following germination. 185 of the 1510 plants flowered before this harvest. Flowering individuals were clustered by RIL (e.g. all ten individuals of RIL 52 flowered whereas no individuals of RIL 53 flowered), though at least one individual from 74 of the RILs flowered. All measurements were made on leaves from non-flowering tillers. Leaf chlorophyll content was estimated by taking the mean value from four leaves measured with a SPAD 502DL Plus spectrophotometer (Spectrum Technologies). Above-ground biomass was excised with a razor blade, dried for 48 h at 80 °C, and weighed. Subsequently the above-ground tissue from one replicate of each RIL in each environment was ground to a fine powder and analyzed for $\delta^{13}\text{C}$, carbon content, and nitrogen content, as described above. The effect of soil drying on measured traits in the RILs was assessed by ANOVA including genotype, treatment, their interaction, and greenhouse block as effects, using the JMP software package. We did not fit a G×E term in the ANOVAs for Leaf N, Leaf C, or $\delta^{13}\text{C}$ because only a single individual of each RIL was measured in each environment for those traits. With the exception of leaf N content, all traits were normally distributed; leaf N values were log-transformed prior to analysis to meet the assumption of normal distribution. We used this analysis to estimate LSMeans for SPAD and biomass values for each RIL in both irrigation treatments. For leaf C, leaf N, and $\delta^{13}\text{C}$ the value of the single replicate plant in each treatment was used. We also used these LSMeans to estimate the genetic correlation between SPAD and biomass traits and between treatments for SPAD and biomass, and the phenotypic correlations between all traits in JMP.

2.4. QTL mapping in Bd3-1 × Bd21 RILs

Following Lowry et al. [58], we used the LSMeans estimates for each measured phenotype to generate two parameters for subsequent QTL scans: the mean of the trait values between the Control and Dry environment measured as (LSMean Dry + LSMean Control)/2, and the plasticity of the trait between environments measured as (LSMean Dry – LSMean Control). Our motivation for this mapping strategy was to identify both QTL that contribute to constitutive (main effect QTL) trait variability as well as QTL affect-

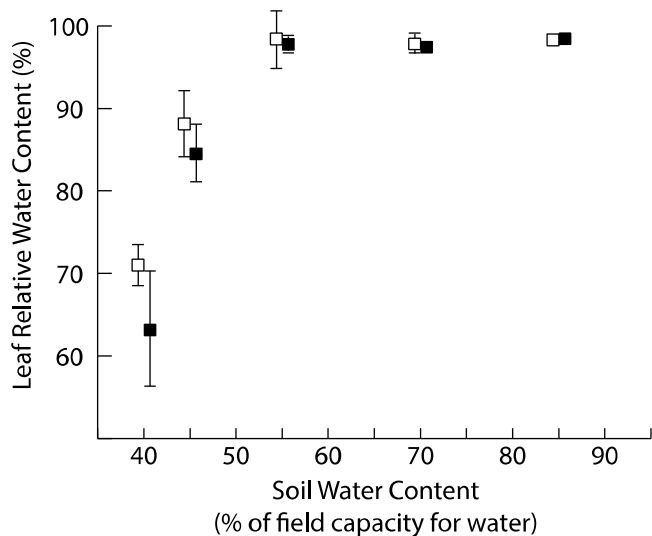


Fig. 1. Leaf relative water content from the growth chamber dry-down. Bd3-1 individuals are shown as black boxes. Bd21 individuals are shown as white boxes. Boxes are “jittered” to ease viewing. Vertical bars indicate one standard error of the mean. $N=4$ for each box.

ing environmentally-induced trait variability (G \times E interaction). We mapped QTL using *r/qtl* version 1.37 (Broman et al. [74]) with both one- and two-dimensional interval mapping using Haley-Knot regression at 1cM steps across the genome. Significance thresholds were determined at an experiment-wide Type 1 error rate of $\alpha=0.1$ using 1000 permutations of the marker dataset. We conducted a forward/backward stepwise search for models with a maximum of five QTL that optimized the penalized LOD score criterion using the stepwise procedure. Confidence intervals for each significant QTL identified in the best-fit models were calculated as the 1.5 LOD drop interval.

We estimated the additive effect of each QTL as half the difference in phenotypic means for the homozygous genotypes at a locus. Here, Bd21 was treated as the reference and so the sign of the additive effect indicates the contribution of the Bd3-1 allele to the estimated trait value (e.g. a negative sign indicates that the Bd3-1 allele decreases the trait mean at that locus). The proportion of total genetic variance explained by each locus, or by interaction between loci (epistasis), was determined using the *fitqtl* function in *r/qtl*.

3. Results and discussion

3.1. Selecting treatment levels and assessing natural diversity of response

We first estimated the progression of plant response to soil drying by measuring leaf relative water content (RWC) along a soil-drying continuum. The results of an ANOVA indicate that our soil-drying resulted in a reduction of leaf RWC as the soil became drier (Fig. 1; ANOVA $F_{\text{HarvestDate} \times \text{WaterTreatment}} = 25.1$, $p < 0.0001$). Visual inspection of Fig. 1 suggests that leaves of *B. distachyon* accession Bd21 and Bd3-1 do not show a reduction in RWC until the soil water content (SWC) is reduced to approximately 50% of field capacity for water. Note that this result does not necessarily indicate that the plants are not responding to soil drying at higher soil water contents; plants have diverse cellular mechanisms to sustain leaf water content in the presence of soil drying, collectively referred to as the dehydration avoidance syndrome [59]. Our results indicate that SWC of approximately 50% may be an inflection point beyond which these two accessions may no longer maintain con-

stant RWC through such mechanisms. We do not observe genetic variation in reduction of RWC during this progressive soil drying (ANOVA $F_{\text{Genotype} \times \text{HarvestDate} \times \text{WaterTreatment}} = 0.056$, $p = 0.982$).

We next assessed the treatment response of Bd21 and Bd3-1 to the strongest drying treatment, contrasting trait values at 85% soil water content (equivalent to 0.54 g H₂O/g soil) with 40% soil water content (equivalent to 0.25 g H₂O/g soil). This SWC resulted in a 28% reduction in leaf RWC compared to the well-irrigated treatment (Supplemental Fig. 1a; ANOVA $F = 92.89$, $p < 0.0001$). Compared to well-watered control plants, dry treatment plants had 17% lower total dry biomass (Supplemental Fig. 1b; ANOVA $F = 5.79$, $p = 0.033$) with a higher root/shootmass ratio (Supplemental Fig. 1c; ANOVA $F = 17.02$, $p = 0.014$). Soil drying also led to higher water use efficiency (WUE, Supplemental Fig. 1d; ANOVA $F = 255.88$, $p < 0.0001$), as measured by a 1.94‰ increase in $\delta^{13}\text{C}$, higher leaf carbon content (Supplemental Fig. 1e; ANOVA $F = 21.63$, $p = 0.0007$), and lower leaf nitrogen content (Supplemental Fig. 1f; ANOVA $F = 33.34$, $p < 0.0001$). The increase in WUE under soil drying is comparable in magnitude to those identified in past studies using both experimentally dried pot-grown *B. distachyon* plants (e.g. [22]) as well as under drought conditions of wheat varieties grown in the field (e.g. [60]). We observed some constitutive genetic diversity in these traits. On average, Bd3-1 plants had 44.9% greater biomass (Supplemental Fig. 1b; ANOVA $F_{\text{Genotype}} = 14.98$, $p = 0.0022$), with higher root/shoot mass ratio (Supplemental Fig. 1c; ANOVA $F = 11.55$, $p = 0.0053$) and lower WUE (Supplemental Fig. 1d; ANOVA $F = 8.50$, $p = 0.0129$) regardless of treatment. No measured traits showed significant genetic variation in response to soil drying (G \times E), although leaf N showed a trend towards greater reduction under soil drying in Bd3-1 as compared to Bd21 (Supplemental Fig. 1f; ANOVA $F_{\text{Genotype} \times \text{Water}} = 4.59$, $p = 0.055$).

3.2. New markers and revised linkage map for the Bd3-1 \times Bd21 RIL population

Cui et al. [40] previously reported a genetic map for the Bd3-1 \times Bd21 mapping population and used it to map a gene associated with resistance to Barley Stripe Mosaic Virus. We updated this linkage map in three ways. First, we identify the approximate physical position of the Cui markers on the most recent release of the Bd21 reference genome. Second, we removed potentially mis-called markers in the Cui dataset by identifying marker assignments that led to the inference of double recombination events over very short map distances. Finally, we identify 150 new genetic markers using reduced-representation genome resequencing of 151 RILs from the population. We combined the “cleaned” Cui markers with our new resequenced markers and present a newly estimated linkage map comprised of 490 markers across 1017 cM, with average inter-marker distance ~ 2 cM (Fig. 2 and Supplemental Table 1). This total map length is shorter than the map previously reported by Cui et al., possibly owing to mis-called markers in the earlier dataset resulting in double recombinants over very short distances, but remains relatively long and highlights the generally high recombination rate in this mapping population [37]. The median inter-marker distance on the physical genome is 272 kilobase pairs. Notable gaps in marker coverage remain between 90.8 and 93.1 cM (~ 6.4 Mbp) and 133.1 and 147.0 (~ 3.2 Mbp) on chromosome 2 and between 35.6 and 44.6 (~ 3.1 Mbp) on chromosome 5. These gaps in marker coverage may simply reflect an absence of nucleotide variants between the Bd21 and Bd3-1 genomes.

This revised and extended linkage map provides several benefits over the existing linkage map available for the Bd3-1 \times Bd21 mapping population. First, the additional markers provide higher resolution for linkage mapping and will facilitate fine-mapping efforts and construction of near isogenic lines. Second, there have been considerable changes in the reference genome sequence fol-

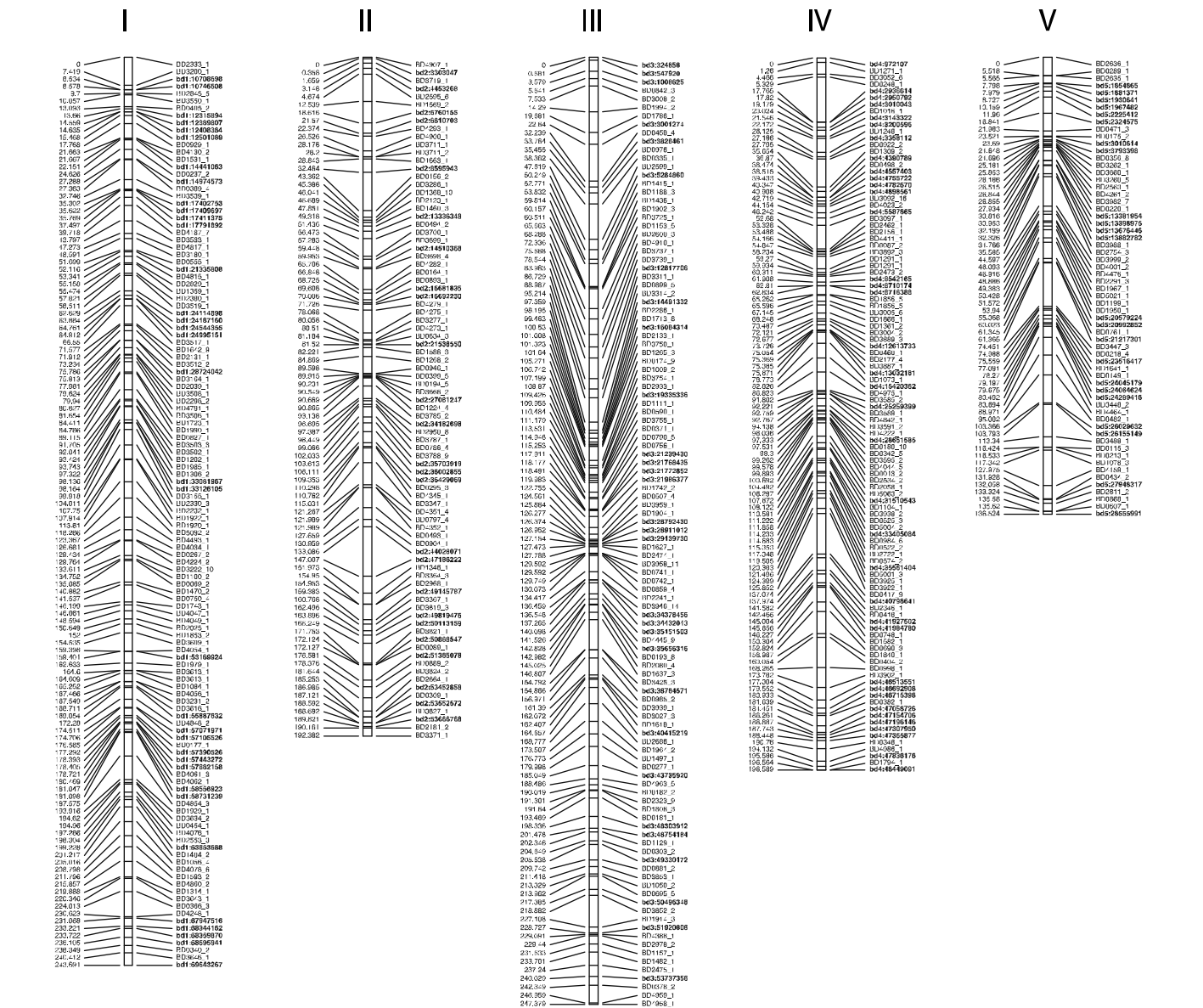


Fig. 2. Graphical representation of the newly estimated linkage map for the Bd3-1 x Bd21 RIL mapping population. Numbers along the left side of linkage groups indicate marker position in cM. Labels along the right side of linkage groups indicate marker names; those in bold are new markers generated in the present study. For new markers, names denote chromosome number before colon and physical position in the *B. distachyon* v3.0 genome is indicated following the colon.

lowing its initial release [36]. By updating the positions of the earlier Cui markers the new map should allow researchers to more readily identify candidate genes associated with genetic loci and exploit the genomic synteny between grass species to identify orthologous loci in temperate cereals. Finally, we have removed possible genotyping errors from the earlier dataset which may have led to reduced statistical power to detect trait-marker associations.

3.3. Quantitative genetics of measured traits in the Bd3-1 x Bd21 RILs

We grew replicates of each of 151 RILs in a controlled-environment greenhouse experiment and exposed plants to either well-watered (control) or restricted-irrigation (dry) treatments. Comparison of the trait means for each parent against the frequencies of line means among RILs reveals that all of our measured traits show considerable transgressive segregation (Fig. 3 and Supporting online Fig. 2). This pattern has been observed previously in other plant species for WUE [21,23,24,26] and plant biomass [24], among

many other traits [61], and indicates that phenotypic variation in the traits is likely due to variation at multiple genetic loci, possibly with parental allelic effects in different directions at each locus which have been recombined among RILs. Transgressive segregation may also indicate epistatic interactions among loci controlling these traits. The range of $\delta^{13}C$ values observed among RILs (-32.65 to -30.17%) is comparable to the difference of 2–3‰ observed among varieties of wheat, barley, rice, and several forage and turf grasses (reviewed by Ref. [13]).

Broad-sense heritabilities of measured traits, measured as the proportion of total phenotypic variance explained by variance among RILs, were appreciable. Heritability for total above ground dry biomass was 0.63 in the well-watered environment and slightly lower, 0.55, in the water-restricted environment. Chlorophyll content, estimated using a SPAD spectrophotometer, was lower than biomass heritabilities: 0.36 in the well-watered environment and 0.43 in the water-restricted environment. Because we only assayed $\delta^{13}C$, leaf C, and leaf N for a single individual of each RIL in each treatment, our sampling scheme precluded us from estimating her-

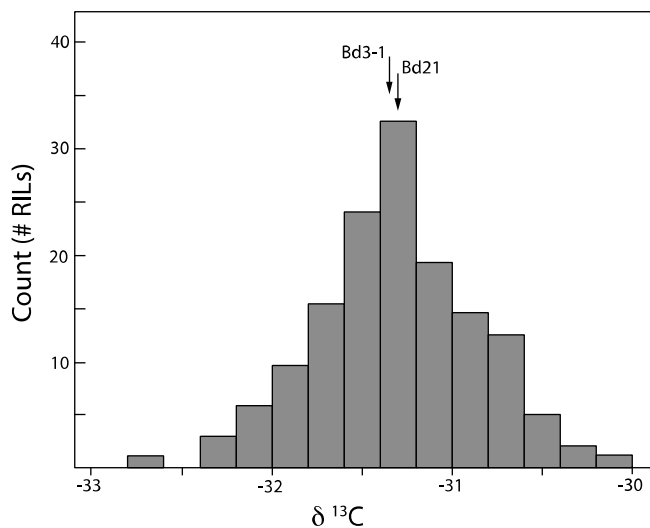


Fig. 3. Frequency distributions of $\delta^{13}\text{C}$ in the Bd21 \times Bd3-1 RIL population. Presented values are the means between the two sampled environments for each RIL. Arrows correspond to the parental line means.

itabilities for these traits; we present a QTL-based approximation of heritable variance for these traits below. In past experiments in wheat, estimated heritabilities for carbon isotope discrimination have generally been quite high, suggesting that G \times E may be moderate for this trait, thus providing high power to detect QTL explaining genetic differences in WUE [32,62].

We observed a strong positive genetic correlation between above ground biomass and leaf chlorophyll content ($\rho=0.58$), which was considerably stronger than the phenotypic correlation between these traits ($\rho=0.26$). Several of the differences in trait means (plasticities) between environments also showed significant, positive phenotypic correlations (Supplemental Table 2). Notably, plasticity in leaf C, leaf N, and $\delta^{13}\text{C}$ are all positively correlated, as is plasticity in leaf C and plasticity in biomass. Collectively, these results suggest that these components of primary metabolism

share a genetic basis in both their constitutive expression and their response to soil drying.

3.4. Effect of drying treatment on traits in the RIL experiment

In our RIL greenhouse experiment, soil drying lead to a significant 23% decrease in plant biomass (Supplemental Fig. 3a; ANOVA $F=265$, $p<0.0001$), a 21% increase in SPAD measurement (Supplemental Fig. 3b; ANOVA $F=285.7$, $p<0.0001$), a 3.0% increase in leaf carbon content (Supplemental Fig. 3c; ANOVA $F=38.1$, $p<0.0001$), and a 24.7% increase in leaf nitrogen content (Supplemental Fig. 3d; ANOVA $F=36.5$, $p<0.0001$; both leaf C and leaf N expressed on a dry leaf weight basis). $\delta^{13}\text{C}$ also increased by 0.42‰ in the dry environment in our greenhouse experiment (Supplemental Fig. 3e; ANOVA $F=50.0$, $p<0.0001$). Representative plants from each treatment are presented in Supplemental Fig. 4.

The observation that leaf N is elevated under soil drying in the greenhouse RIL experiment conflicts with the observed decrease in leaf N under drying in the growth chamber experiment, described above. Regardless of experimental treatment, leaf N concentrations were substantially lower in the greenhouse-grown plants as compared to chamber grown plants (cf. Supplemental Figs. 1f and 3d). There were several important differences between the greenhouse and chamber experiments, notably that the greenhouse plants received considerably higher light levels of different quality (natural sunlight vs. artificial broad-spectrum fluorescence) and that the greenhouse plants were older at harvest (54 days post germination compared to 30 days in the chamber experiment). The elevated leaf N under water-restriction, observed in the greenhouse, is consistent with results from our earlier work in *A. thaliana* in which the increase in leaf N was correlated with a transcriptional signature of increased investment in photosynthetic machinery [4]. We interpreted the increase in leaf N as signifying changes in photosynthetic capacity, perhaps related to increased carbon acquisition directed towards root growth as a dehydration avoidance response.

3.5. Identifying QTL associated with plant-water relations

Our analysis of the greenhouse-grown Bd3-1 \times Bd21 RILs provides two key results which improve our understanding of the

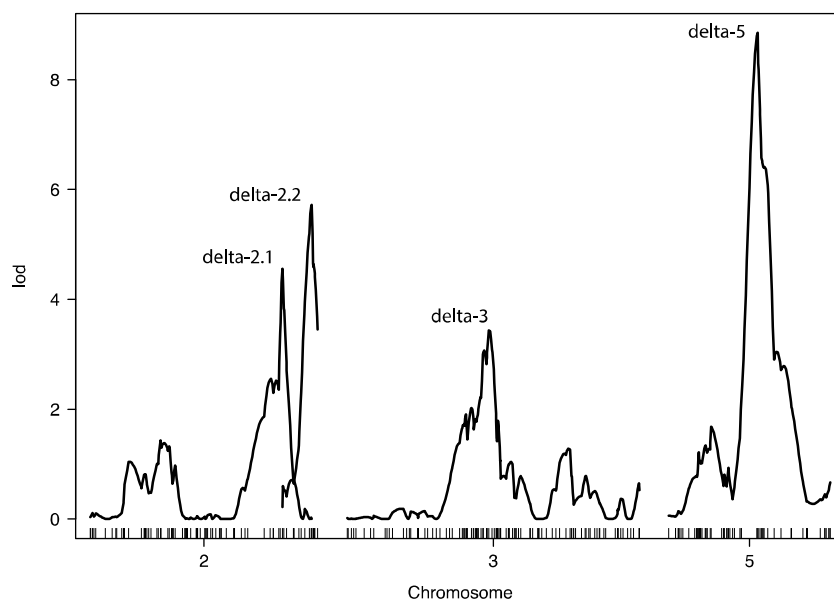


Fig. 4. Conditional QTL LOD plot for $\delta^{13}\text{C}$ as estimated using stepwise regression in r/qtl . Mapped $\delta^{13}\text{C}$ values are the mean between the two sampled environments. Named LOD peaks are significant at $\alpha=0.1$, as determined by permutation testing. Only chromosomes with a significant QTL association are shown. Details on effect size for each QTL are presented in Table 1.

Table 1
Results of QTL analyses in the Bd3-1 × Bd21 population using two-dimensional genome scans.

QTL	Trait	Chrom.	Position (cM)(1.5 LOD CI)	Nearest marker	Effect 2a (s.e)	%V _G
Delta-2.1	δ ¹³ C	2	162.5 (160–166)	BD3819.3	−0.154 (0.033)	9.3
Delta-2.2	δ ¹³ C	2	187.1 (182–191)	BD0309.1	−0.040 (0.033)	11.9
Delta-3	δ ¹³ C	3	120.0 (104–125.9)	BD3:21986377	0.120 (0.030)	6.9
Delta-5	δ ¹³ C	5	75.0 (70–78)	BD0218.4	0.139 (0.030)	19.4
leafCdiff-1	Leaf C Plasticity	1	176.0 (156–187)	BD0177.1	−5.770 (1.418)	10.0
Biomass-1	Total aerial dry biomass	1	98 (90–112)	BD1:33081967	0.062 (0.017)	7.3
Biomass-2	Total aerial dry biomass	2	89.9 (83–114)	BD0399.5	0.066 (0.017)	8.5

genetic basis of plant-water relations in *B. distachyon* and grasses, more generally. First, we identify six QTL explaining constitutive trait variation between Bd21 and Bd3-1 (Table 1). In this analysis of constitutive-effect QTL, we used the mean trait value between the two sampled environments in model fitting. Four of these constitutive QTL are associated with WUE, measured here as carbon isotope discrimination (δ¹³C); we assign the prefix “delta” for these δ¹³C QTL (Fig. 4). Collectively, the four δ¹³C QTL explain 37.5% of the total genetic variance in δ¹³C in the mapping population. In the absence of a direct estimate for heritability of WUE, this percent of variance explained by the four QTL gives an approximation of the proportion of phenotypic variance that can be explained by the detected genetic factors. The additive effect of these δ¹³C QTL are generally larger than observed previously in field-grown wheat mapping populations [24], though comparable in magnitude to the effects of loci identified in a greenhouse-grown rice population [26]. As predicted by the transgressive segregation observed for δ¹³C, the additive effects of parental alleles differ in magnitude and direction among loci, with Bd3-1 alleles at delta-2.1 and delta-2.2 reducing δ¹³C values and those at delta-3.1 and delta-5.1 increasing δ¹³C values. We also find that two QTL, delta-5 and delta-2.2, interact epistatically (Fig. 5; results of the full stepwise QTL model for this interaction LOD = 5.325, *p* < 0.001). The epistatic interaction between these two QTL explains 11.03% of the variance in WUE in the Bd3-1 × Bd21 cross.

Notably, we do not observe any QTL which describe phenotypic difference in δ¹³C between the control and restricted-irrigation environments, indicating that there are no QTL for plasticity in δ¹³C. This suggests that the genetic architecture controlling WUE in *B. distachyon* may be relatively canalized. Rebetzke et al. [24] previously reported similarly strong constitutive effects of QTL controlling δ¹³C in several varieties of wheat grown in multiple experimental field plots of wheat, which contrasted with the strong G×E observed

for yield and biomass in that experiment. Note that neither our results, nor those reported previously for wheat, reject the hypothesis that WUE is a plastic trait: numerous studies have shown that soil drying generally leads to increased WUE [22,60,63,64] and we also observed this pattern in both our chamber and greenhouse experiments. Indeed, G×E for WUE has been detected in several grass species [65,66].

The absence of plasticity QTL for δ¹³C indicates that the largest-effect QTL in the Bd3-1 × Bd21 cross are generally insensitive to environmental change and suggests that what G×E exists for WUE may be controlled by loci of generally smaller effect. WUE plasticity loci may also have complex patterns of inheritance – such as dominance, epistasis, tightly linked loci of opposing allelic effect, etc. – that make detecting their genetic basis experimentally challenging. An important caveat for our study is that we have sampled limited genetic diversity – just two accessions from modern-day Iraq – and so absence of G×E for WUE or other traits may not reflect patterns observed in larger panels of natural accessions; a recent study using a larger panel of *B. distachyon* natural accessions revealed extensive G×E for WUE [22].

We also identify two QTL associated with genetic variability in total above-ground dry biomass. Again, here we fit the mean above ground biomass between the two sampled environments. These QTL are of relatively small effect, with the Bd21 allele at the biomass-2 locus leading to larger plants at both loci. Of note, Bd3-1 is a larger plant than Bd21 under a range of environmental conditions [45,46] so it is perhaps surprising that we did not detect more QTL describing this phenotypic difference. A possible explanation for this discrepancy is that biomass may be controlled by many loci of small effect which were not detected in our mapping efforts. The observation that our best-fit qtl model explains a small fraction of observed heritable genetic variation support this hypothesis: the two detected QTL explain just 16% of genetic variance whereas our

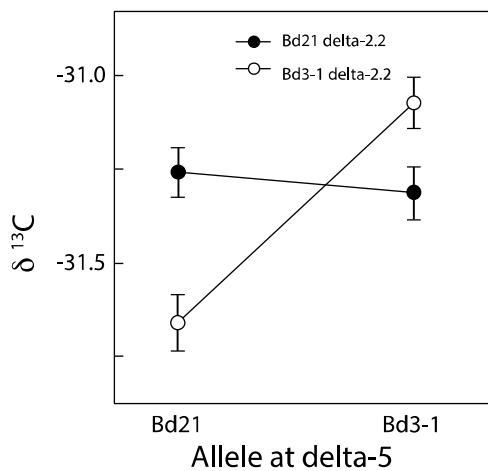


Fig. 5. Epistatic interactions between δ¹³C QTL detected on linkage group 2 (delta-2.2) and linkage group 5 (delta-5) detected in stepwise regression genome scans. Mapped δ¹³C values are the mean between the two sampled environments. Vertical bars indicate one standard error of the mean.

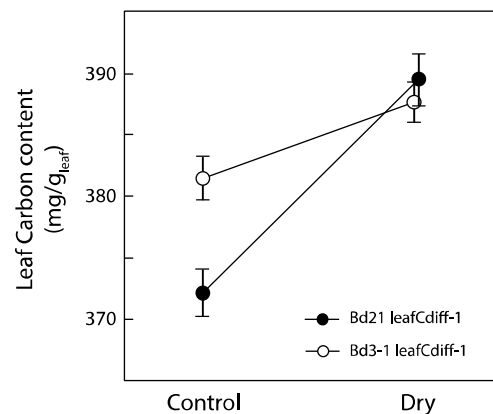


Fig. 6. Reaction norm plot showing plastic leaf carbon content controlled by a locus on linkage group 1 (leafCdiff-1) detected in stepwise regression genome scans. “Control” treatment plants received 100 mL of water every second day while “Dry” treatment plants received 50 mL of water every second day. Vertical bars indicate one standard error of the mean.

estimate of heritability for above ground biomass was over 0.5 in both sampled environments.

The second observation from our mapping analysis is the presence of an environmentally-dependent QTL (indicating G×E; mapped on the difference between dry and wet environments) for leaf carbon content on chromosome 1. This environmental effect is due to a genetic difference in leaf C content in the wet environment that is absent in the dry environment (Fig. 6; results of the full stepwise QTL model for this interaction LOD = 3.46, $p < 0.001$), a genetic architecture called conditional neutrality [67]. Conditionally-neutral genetic loci are of potential interest for plant breeding because the beneficial effects of an allele in one environment – here, relatively greater leaf C conferred by the Bd3-1 allele when water is plentiful – is not associated with a difference in trait values in a second environment.

We do not detect QTL for leaf N or SPAD at an experiment-wide $\alpha = 0.1$. As noted above, heritabilities for SPAD were relatively lower than for above ground biomass, indicating a greater contribution of environmental factors in explaining experimental variance. These low heritabilities may have prevented us from detecting QTL for this trait.

One striking result from our QTL analysis is that we observe significant phenotypic correlations among several of our traits (Supplemental Table 2), though none of the QTL detected at $\alpha = 0.1$ overlap with another QTL (e.g. the 1.5 LOD intervals around QTL peaks do not overlap). One explanation for this observation is that the traits studied here are controlled by additional loci of small effect, possibly in an environmentally-dependent manner, leaving us with little statistical power to detect QTL and thereby little power to detect co-localization of QTL for different traits [68,69].

3.6. Concluding remarks

Plant responses to soil drying are complex, involving changes in primary and secondary metabolism, biomass partitioning, cell wall composition, transpiration, and hydraulic adjustments, to name but a few. These responses vary substantially within and between species, and according to the duration, developmental timing, and severity of stress. This experimental and genetic variation has complicated efforts to develop a clear picture of what responses are truly adaptive—i.e. favored by natural selection to increase fitness under stressful conditions. In particular, interpreting the effects of water limitation on primary metabolic activity and photosynthate partitioning is an enduring challenge [70]. Several recent studies in *A. thaliana* shed light on this key issue, revealing that moderate soil drying – similar to the stress imposed here – increases plant carbon status as revealed by transcriptional signature of elevated carbon assimilation and high leaf C and leaf N content [4,71,72]. Recent work in *B. distachyon* (Bd21 accession) likewise found no transcriptional signature of carbon limitation and, in fact, observed that leaf cell division continued unabated during soil drying though cell expansion was significantly curtailed [73]. This “wait and see” growth response to stressful conditions may be favored in environments with unpredictable rainfall during the growing season.

Our greenhouse results are consistent with these earlier studies. First, we observe elevated leaf C, N, and SPAD readings under moderate soil drying, all consistent with the hypothesis that these plants remain photosynthetically active. While we did not measure root-shoot biomass ratios in the greenhouse experiment, our chamber experiment revealed increased relative investment in root tissue, which is a frequently observed response to soil drying that would require sustained carbon assimilation in this short-lived annual species.

The QTL which detected here represent an important first step in identifying the molecular basis of WUE, leaf carbon content, and plant biomass in this model grass species. Importantly, unlike

genetic loci identified via gene artificial mutagenesis screens, the variants discovered by QTL mapping are viable in the field (by virtue of existing in wild-collected accessions) and therefore may reveal orthologous loci which are amenable to manipulative breeding in crop species. Our revised genetic map for the Bd3-1 × B21 mapping population may prove useful for this translational approach. The conditionally-neutral allele which we identified for leaf carbon content may be of particular interest, in this regard, as conditionally neutral alleles can circumvent the problems associated with yield-drag when breeding for yield in specific environments [67].

Acknowledgements

Colin Purmal, Kathleen Burns, Emeline Sukamtoh, Omar Gonzales, and Erin Atkinson assisted with RIL phenotyping. Tierney Logan extracted DNA and prepared the SOLiD libraries for sequencing. Comments from E. Blumwald and two anonymous reviewers greatly improved the manuscript. This work was supported by a USDA NIFA award (2011-67012-30663) to D.L.D., an NSF Postdoctoral Research Fellowship (DBI-1103668) to K.M.H, USDA CRIS Project Award (5062-21000-030-00D) to D.F.G., and an NSF Plant Genome Research Program award (IOS-0922457) to T.E.J.

Appendix A. Supplementary data

Supplementary data associated with this article can be found, in the online version, at <http://dx.doi.org/10.1016/j.plantsci.2016.03.010>.

References

- [1] H.J. Bohnert, D.E. Nelson, R.G. Jensen, Adaptations to environmental stresses, *Plant Cell* 7 (1995) 1099–1111.
- [2] G.L. Stebbins, Aridity as a stimulus to plant evolution, *Am. Nat.* 86 (1952) 33–44.
- [3] R.H. Whittaker, *Communities and Ecosystems*, 2nd ed., Macmillan, New York, 1975.
- [4] D.L. Des Marais, J.K. McKay, J.H. Richards, S. Sen, T. Wayne, T.E. Juenger, Physiological genomics of response to soil drying in diverse *Arabidopsis* accessions, *Plant Cell* 24 (2012) 893–914.
- [5] L.A. Donovan, S.A. Dudley, D.M. Rosenthal, F. Ludwig, Phenotypic selection on leaf water use efficiency and related ecophysiological traits for natural populations of desert sunflower, *Oecologia* 152 (2007) 13–25.
- [6] H.M. Easlon, K.S. Nemali, J.H. Richards, D.T. Hanson, T.E. Juenger, J.K. McKay, The physiological basis for genetic variation in water use efficiency and carbon isotope composition in *Arabidopsis thaliana*, *Photosynth. Res.* 119 (2014) 119–129.
- [7] M.A. Geber, T. Dawson, Genetic variation in stomatal and biochemical limitations to photosynthesis in the annual plant, *Polygonum arenastrum*, *Oecologia* 109 (1997) 535–546.
- [8] M.S. Heschel, K. Donohue, N. Hausmann, J. Schmitt, Population differentiation and natural selection for water-use efficiency in *Impatiens capensis* (Balsaminaceae), *Int. J. Plant Sci.* 163 (2002) 907–912.
- [9] K.T. Hubick, G.D. Farquhar, Carbon isotope discrimination and the ratio of carbon gained to water lost in barley cultivars, *Plant Cell Environ.* 12 (1989) 795–804.
- [10] J.E. Quisenberry, B.L. McMichael, Genetic variation among cotton germplasm for water-use efficiency, *Environ. Exp. Bot.* 31 (1991) 433–460.
- [11] R. Van den Boogard, D. Alewijnse, E.J. Veneklaas, H. Lambers, Growth and water-use efficiency of 10 *Triticum aestivum* cultivars at different water availability in relation to allocation of biomass, *Plant Cell Environ.* 20 (1997) 200–210.
- [12] H. Lambers, F.S. Chapin III, T.L. Pons, *Plant Physiological Ecology*, 2nd ed., Springer, New York, NY, 2008.
- [13] A.G. Condon, G.D. Farquhar, G.J. Rebetzke, R.A. Richards, The application of carbon isotope discrimination in cereal improvement for water-limited environments, in: J.M. Ribaut (Ed.), *Drought Adaptation in Cereals*, Haworth Press, Inc., New York, NY, 2006, pp. 171–219.
- [14] G.D. Farquhar, R.A. Richards, Isotopic composition of plant carbon correlates with water-use efficiency of wheat genotypes, *Aust. J. Plant Physiol.* 11 (1984) 539–552.
- [15] G.D. Farquhar, J.R. Ehleringer, K.T. Hubick, Carbon isotope discrimination and photosynthesis, *Annu. Rev. Plant Physiol. Plant Mol. Biol.* 40 (1989) 503–538.
- [16] J.P. Comstock, S.R. McCouch, B.C. Martin, C.G. Tauer, T.J. Vision, Y. Xu, R.C. Pausch, The effects of resource availability and environmental conditions on

- genetic rankings for carbon isotope discrimination during growth in tomato and rice, *Funct. Plant Biol.* 32 (2005) 1089–1105.
- [17] J.K. McKay, J.H. Richards, T. Mitchell-Olds, Genetics of drought adaptation in *Arabidopsis thaliana*: I. Pleiotropy contributes to genetic correlations among ecological traits, *Mol. Ecol.* 12 (2003) 1137–1151.
- [18] F. Vasseur, T. Bontpart, M. Dauzat, C. Granier, D. Vile, Multivariate genetic analysis of plant responses to water deficit and high temperature revealed contrasting adaptive strategies, *J. Exp. Bot.* 65 (2014) 6457–6469.
- [19] A.P. Dhanapal, J.D. Ray, S.K. Singh, V. Hoyos-Villegas, J.R. Smith, L.C. Purcell, C.A. King, P.B. Cregan, Q. Song, F.B. Fritschi, Genome-wide association study (GWAS) of carbon isotope ratio ($\delta^{13}C$) in diverse soybean [*Glycine max* (L.) Merr.] genotypes, *Theor. Appl. Genet.* 128 (2015) 73–91.
- [20] N.J. Hausmann, T.E. Juenger, S. Sen, K.A. Stowe, T.E. Dawson, E.L. Simms, Quantitative trait loci affecting $\delta^{13}C$ and response to differential water availability in *Arabidopsis thaliana*, *Evolution* 59 (2005) 81–96.
- [21] T.E. Juenger, J. McKay, N. Hausmann, J. Keurentjes, S. Sen, K. Stowe, T. Dawson, E. Simms, J. Richards, Identification and characterization of QTL underlying whole-plant physiology in *Arabidopsis thaliana*: $\delta^{13}C$ stomatal conductance and transpiration efficiency, *Plant Cell Environ.* 28 (2005) 697–708.
- [22] A.J. Manzaneda, P.J. Rey, J.T. Anderson, E. Raskin, C. Weiss-Lehman, T. Mitchell-Olds, Natural variation, differentiation and genetic tradeoffs of ecophysiological traits in response to water limitation in *Brachypodium distachyon* and its descendent allotetraploid *B. hybridum* (Poaceae), *Evolution* 69 (2015) 2689–2704.
- [23] J.K. McKay, J.H. Richards, K.S. Nemali, S. Sen, T. Mitchell-Olds, S. Boles, E.A. Stahl, T. Wayne, T.E. Juenger, Genetics of drought adaptation in *Arabidopsis thaliana* II. QTL analysis of a new mapping population, KAS-1 \times TSU-1, *Evolution* 62 (2008) 3014–3026.
- [24] G.J. Rebetzke, A.G. Condon, G.D. Farquhar, R. Appels, R.A. Richards, Quantitative trait loci for carbon isotope discrimination are repeatable across environments and wheat mapping populations, *Theor. Appl. Genet.* 118 (2008) 123–137.
- [25] X. Xu, B. Martin, J.P. Comstock, T.J. Vision, C.G. Tauer, B. Zhao, R.C. Pausch, S. Knapp, Fine mapping a QTL for carbon isotope composition in tomato, *Theor. Appl. Genet.* 117 (2008) 221–233.
- [26] Y. Xu, D. This, R.C. Pausch, W.M. Vonhof, J.R. Coburn, J.P. Comstock, S.R. McCouch, Leaf-level water use efficiency determined by carbon isotope discrimination in rice seedlings: genetic variation associated with population structure and QTL mapping, *Theor. Appl. Genet.* 118 (2009) 1065–1081.
- [27] J.T. Lovell, T.E. Juenger, S.D. Michaels, J.R. Lasky, A. Platt, J.H. Richards, X. Yu, H.M. Easlon, S. Sen, J.K. McKay, Pleiotropy of FRIGIDA enhances the potential for multivariate adaptation, *Proc. Biol. Sci.* 280 (2013) 20131043.
- [28] J. Masle, S.R. Gilmore, G.D. Farquhar, The *ERECTA* gene regulates plant transpiration efficiency in *Arabidopsis*, *Nature* 436 (2005) 866–870.
- [29] D.L. Des Marais, L.C. Auchincloss, E. Sukamtoh, J.K. McKay, T. Logan, J.H. Richards, T.E. Juenger, Variation in MPK12 affects water use efficiency in *Arabidopsis* and reveals a pleiotropic link between guard cell size and ABA response, *Proc. Natl. Acad. Sci. U. S. A.* 111 (2014) 2836–2841.
- [30] P. Monneveux, R. Jing, S.C. Misra, Phenotyping for drought adaptation in wheat using physiological traits, *Front. Physiol.* 3 (2012) 429.
- [31] R. Tuberosa, Mapping QTLs regulating morpho-physiological traits and yield: case studies, shortcomings and perspectives in drought-stressed maize, *Ann. Bot.* 89 (2002) 941–963.
- [32] G.J. Rebetzke, A.G. Condon, R.A. Richards, G.D. Farquhar, Selection for reduced carbon isotope discrimination increases aerial biomass and grain yield of rainfed bread wheat, *Crop Sci.* 42 (2002) 739–745.
- [33] B.E. Campitelli, D.L. Des Marais, T.E. Juenger, Ecological interactions and the fitness effect of water-use efficiency: competition and drought alter the impact of natural MPK12 alleles in *Arabidopsis*, *Ecol. Lett.* 19 (2016) 424–434.
- [34] P. Catalan, J. Muller, R. Hasterok, G. Jenkins, L.A. Mur, T. Langdon, A. Betekhtin, D. Siwinska, M. Pimentel, D. Lopez-Alvarez, Evolution and taxonomic split of the model grass *Brachypodium distachyon*, *Ann. Bot.* 109 (2012) 385–405.
- [35] J. Vogel, Genetics and genomics of *Brachypodium*, in: R. Jorgensen (Ed.), *Plant Genetics and Genomics: Crop Models*, Springer, 2016.
- [36] The International Brachypodium Initiative, Genome sequencing and analysis of the model grass *Brachypodium distachyon*, *Nature* 463 (2010) 763–768.
- [37] D.F. Garvin, *Brachypodium distachyon* genetic resources, in: J. Vogel (Ed.), *Genetics and Genomics of Brachypodium*, Springer, 2016.
- [38] S. Gordon, H. Priest, D.L. Des Marais, W. Schackwitz, M. Figueroa, J. Martin, J. Bragg, L. Tyler, C.-R. Lee, D. Bryant, W. Wang, J. Messing, A. Manzaneda, K. Barry, D. Garvin, H. Budak, M. Tuna, T. Mitchell-Olds, W. Pfender, T. Juenger, T.C. Mockler, J. Vogel, Genome diversity in *Brachypodium distachyon*: deep sequencing of highly diverse inbred lines, *Plant J.* 79 (2014) 361–374.
- [39] C.J. Schwartz, M.R. Doyle, A.J. Manzaneda, P.J. Rey, T. Mitchell-Olds, R.M. Amasino, Natural variation of flowering time and vernalization responsiveness in *Brachypodium distachyon*, *Bioenergy Res.* 3 (2010) 38–46.
- [40] Y. Cui, M.Y. Lee, N. Huo, J. Bragg, L. Yan, C. Yuan, C. Li, S.J. Holditch, J. Xie, M.-C. Luo, D. Li, J. Yu, J. Martin, W. Schackwitz, Y.Q. Gu, J.P. Vogel, A.O. Jackson, Z. Liu, D.F. Garvin, Fine mapping of the *Bsr1* barley stripe mosaic virus resistance gene in the model grass *Brachypodium distachyon*, *PLoS One* 7 (2012) e38333.
- [41] V. Chochois, J. Vogel, G.J. Rebetzke, M. Watt, Variation in adult plant phenotypes and partitioning among seed and stem-borne roots across *Brachypodium distachyon* accessions to exploit in breeding cereals for well-watered and drought environments, *Plant Physiol.* 168 (2015) 953–967.
- [42] K. Colton-Gagnon, M.A. Ali-Benali, B.F. Mayer, R. Dionne, A. Bertrand, S. Do Carmo, J.B. Charron, Comparative analysis of the cold acclimation and freezing tolerance capacities of seven diploid *Brachypodium distachyon* accessions, *Ann. Bot.* 113 (2014) 681–693.
- [43] E. Filiz, B.S. Ozdemir, F. Budak, J.P. Vogel, M. Tuna, H. Budak, Molecular, morphological and cytological analysis of diverse *Brachypodium distachyon* inbred lines, *Genome* 52 (2009) 876–890.
- [44] P.A. Ingram, J. Zhu, A. Shariff, I.W. Davis, P.N. Benfey, T. Elich, High-throughput imaging and analysis of root system architecture in *Brachypodium distachyon* under differential nutrient availability, *Philos. Trans. R. Soc. Lond. Ser. B Biol. Sci.* 367 (2012) 1559–1569.
- [45] N. Luo, J. Liu, X. Yu, Y. Jiang, Natural variation of drought response in *Brachypodium distachyon*, *Physiol. Plant.* 141 (2011) 19–29.
- [46] L. Tyler, J.U. Fangel, A.D. Fagerström, M.A. Steinwand, T.K. Raab, W.G.T. Willats, J.P. Vogel, Selection and phenotypic characterization of a core collection of *Brachypodium distachyon* inbred lines, *BMC Plant Biol.* 14 (2014) 25.
- [47] A.J. Kelly, J.H. Willis, Polymorphic microsatellite loci in *Mimulus guttatus* and related species, *Mol. Ecol. Notes* 7 (1998) 769–774.
- [48] S. Wang, E. Meyer, J.K. McKay, M.V. Matz, 2b-RAD: a simple and flexible method for genome-wide genotyping, *Nat. Methods* 9 (2012) 808–810.
- [49] M. David, M. Dzamba, D. Lister, L. Ilie, M. Brudno, SHRIMP2: sensitive yet practical short read mapping, *Bioinformatics* 27 (2011) 1011–1012.
- [50] A. Tarasov, A.J. Vilella, E. Cuppen, I.J. Nijman, P. Prins, Sambamba: fast processing of NGS alignment formats, *Bioinformatics* (2015) btv098.
- [51] A. McKenna, M. Hanna, E. Banks, A. Sivachenko, K. Cibulskis, A. Kernysky, K. Garimella, D. Altshuler, S. Gabriel, M. Daly, M.A. DePristo, The Genome Analysis Toolkit: a MapReduce framework for analyzing next-generation DNA sequencing data, *Genome Res.* 20 (2010) 1297–1303.
- [52] G.A.V. de Auwera, M.O. Carneiro, C. Hartl, R. Poplin, G. del Angel, A. Levy-Moonshine, T. Jordan, K. Shakir, D. Roazen, J. Thibault, E. Banks, K.V. Garimella, D. Altshuler, S. Gabriel, M.A. DePristo, From fastq data to high-confidence variant calls: the genome analysis toolkit best practices pipeline, *Curr. Protoc. Bioinform.* 11 (2013) 11.10.11–11.10.33.
- [53] D.B. Lowry, K. Hernandez, S.H. Taylor, E. Meyer, T.L. Logan, K.W. Barry, J.A. Chapman, D.S. Rokhsar, J. Schmutz, T.E. Juenger, The genetics of divergence and reproductive isolation between ecotypes of *Panicum hallii*, *New Phytol.* 205 (2015) 402–414.
- [54] E. Garrison, G. Marth, Haplotype-based variant detection from short-read sequencing, *arXiv preprint* (2012) 1207.3907.
- [55] A. Tan, G.R. Abecasis, H.M. Kang, Unified representation of genetic variants, *Bioinformatics* 31 (2015) 2202–2204.
- [56] C. Camacho, G. Coulouris, V. Avagyan, N. Ma, J. Papadopoulos, K. Bealer, T.L. Madden, BLAST+: architecture and applications, *BMC Bioinformatics* 10 (2009) 421.
- [57] J.W. Van Ooijen, JoinMap 4, Software for the Calculation of Genetic Linkage Maps in Experimental Populations, Kyazma B.V., Wageningen, Netherlands, 2006.
- [58] D.B. Lowry, T.L. Logan, L. Santuari, C.S. Hardtke, J.H. Richards, L.J. DeRose-Wilson, J.K. McKay, S. Sen, T.E. Juenger, Expression quantitative trait locus mapping across water availability environments reveals contrasting associations with genomic features in *Arabidopsis*, *Plant Cell* 25 (2013) 3266–3279.
- [59] M.M. Ludlow, Strategies of response to water stress, in: K.H. Kreeb, H. Richter, T.M. Hinckley (Eds.), *Structural and Functional Responses to Environmental Stresses*, SPB Academic, The Hague, 1989, pp. 269–281.
- [60] O. Merah, E. Deleens, P. Monneveux, Grain yield carbon isotope discrimination, mineral and silicon content in durum wheat under different precipitation regimes, *Crop Sci.* 107 (1999) 387–394.
- [61] L.H. Rieseberg, A. Widmer, A.M. Arntz, J.M. Burke, The genetic architecture necessary for transgressive segregation is common in both natural and domesticated populations, *Philos. Trans. R. Soc. Lond. B Biol. Sci.* 358 (2003) 1141–1147.
- [62] G.J. Rebetzke, R.A. Richards, A.G. Condon, G.D. Farquhar, Inheritance of carbon isotope discrimination in bread wheat, *Euphytica* 150 (2006) 97–106.
- [63] A.G. Condon, R.A. Richards, G.D. Farquhar, The effect of variation in soil water availability, vapour pressure deficit, and nitrogen nutrition on carbon isotope discrimination in wheat, *Aust. J. Agric. Res.* 43 (1992).
- [64] D. Rengel, S. Arribat, P. Maury, M.L. Martin-Magniette, T. Hourlier, M. Laporte, D. Vares, S. Carrere, P. Grieu, S. Balzergue, J. Gouzy, P. Vincourt, N.B. Langlade, A gene-phenotype network based on genetic variability for drought responses reveals key physiological processes in controlled and natural environments, *PLoS One* 7 (2012) e45249.
- [65] Z. Peleg, T. Fahima, S. Abbo, T. Krugman, E. Nevo, D. Yakir, Y. Saranga, Genetic diversity for drought resistance in wild emmer wheat and its ecogeographical associations, *Plant Cell Environ.* 2 (2005) 176–191.
- [66] D. Robinson, L.L. Handley, C.M. Scrimgeour, D.C. Gordon, B.P. Forster, R.P. Ellis, Using stable isotope natural abundances ($\delta^{15}N$ and $\delta^{13}C$) to integrate the stress responses of wild barley (*Hordeum spontaneum* C. Koch) genotypes, *J. Exp. Bot.* 51 (2000) 41–50.
- [67] D.L. Des Marais, K.H. Hernandez, T.E. Juenger, Genotype-by-environment interaction and plasticity: exploring genomic responses of plants to the abiotic environment, *Annu. Rev. Ecol. Syst.* 44 (2013) 5–29.
- [68] G. Gibson, Rare and common variants: twenty arguments, *Nat. Rev. Genet.* 13 (2012) 135–145.
- [69] M.V. Rockman, The QTN program and the alleles that matter for evolution: all that's gold does not glitter, *Evolution* 66 (2012) 1–17.

- [70] C. Pinheiro, M.M. Chaves, Photosynthesis and drought: can we make metabolic connections from available data? *J. Exp. Bot.* 62 (2011) 869–882.
- [71] I. Hummel, F. Pantin, R. Sulpice, M. Piques, G. Rolland, M. Dauzat, A. Christophe, M. Pervent, M. Bouteillé, M. Stitt, Y. Gibon, B. Muller, Arabidopsis plants acclimate to water deficit at low cost through changes of carbon usage: an integrated perspective using growth, metabolite, enzyme, and gene expression analysis, *Plant Physiol.* 154 (2010) 357–372.
- [72] A. Skirycz, S. De Bodt, T. Obata, I. De Clercq, H. Claeys, R. De Rycke, M. Andriankaja, O. Van Aken, F. Van Breusegem, A.R. Fernie, D. Inze, Developmental stage specificity and the role of mitochondrial metabolism in the response of Arabidopsis leaves to prolonged mild osmotic stress, *Plant Physiol.* 152 (2010) 226–244.
- [73] W. Verelst, E. Bertolini, S. De Bodt, K. Vandepoele, M. Demeulenaere, M.E. Pe, D. Inze, Molecular and physiological analysis of growth-limiting drought stress in *Brachypodium distachyon* leaves, *Mol Plant* 6 (2013) 311–322.
- [74] K.W. Broman, H. Wu, S. Sen, G.A. Churchill, R/qtl: QTL mapping in experimental crosses, *Bioinformatics* 19 (2003) 889–890.